COMBUSTION TEST OF A MICRO CAN TYPE COMBUSTOR FOR MEMS GAS TURBINE ENGINES

Akira FURUTANI[1], Yu SUZUKI[1], Shouhei OZEKI[2], Cholho KIM[2], Naoki TAKANO[3], Naoki MATSUZUKA[1] and Toshiyuki TORIYAMA[1]

[1]Department of Micro System Technology, Ritsumeikan University, 1-1-1 Nojihigashi, Kusatsu, Shiga, Japan

[2]Software CRADLE Co., Ltd,. 3-4-5 Umeda, Kitaku, Osaka, Japan

[3]Department of Mechanical Engineering, Keio University, 3-14-1 Hiyoshi, Kohoku-ku, Yokohama, Kanagawa, Japan

Abstract: This paper describes the design of a can type combustor (hereafter we call "micro combustor") and the result of combustion test for MEMS gas turbine engines. The micro combustor has dimensions of 23.5 x 38.75 x 3.5 mm^3 in width, length and height, respectively. The combustion chamber was designed in detail by using chemical reactor theory and fabricated by MEMS processes. The results of the combustion test show that stable combustion was sustained inside combustion chamber. These results were plotted within the stable combustion of stability map for the micro combustor derived by the chemical reactor theory.

Key words: micro combustor, chemical reactor theory, CLP, MEMS

1. INTRODUCTION

Recently, micro heat engines are being studied for the power generation system of potable electronics, micro robots, miniaturized vehicles and micro satellites. Micro heat engines are divided into three types, gas turbine, reciprocating and Wankel engines. Gas turbine engines have higher output weight ratio than the other ones, and can obtain high output power, which is a very attractive for a micro power generation system. The problems to miniaturize gas turbine engines are as follows; (1) total pressure loss becomes higher in a compressor because of an increase of the heat transfer, (2) heat loss increases with an increase of the surface area to volume ratio, and (3) volume ratio of a combustor to an entire engine becomes larger.

So far, Massachusetts Institute of Technology and SIMTEC have studied the silicon (Si)-based micro gas turbine engine [1, 2], and the research for a three-dimensional palmtop gas turbine engine is demonstrated in Tohoku University [3]. These gas turbine engines employ an annular type combustor, and have an advantage in its miniaturization. This type of the combustor, however, tends to transfer the generated heat toward the compressor and increase the surface area to volume ratio. Thus, this type has the problem described in (1) and (2). A can type combustor is a good candidate for overcoming these problems. This combustor should be designed to give the chamber volume for stable combustion as small as possible, in order to resolve the remaining problem of (3).

The objective of this research is to establish the design of the chamber for the small scale can type combustor by applying the chemical reactor theory used in conventional large scale combustors, and to estimate combustion chamber volume required for stable combustion. Finally, the validity of the design concept is verified by combustion tests.

2. COMBUSTOR STRUCTURE

Figure 1 shows the schematic of micro combustor structure and gas passage. The combustor consists of several Si layers. The models of seven layers and five layers are designed in this research. The combustor with the seven layers has dimensions of 23.5 mm x 38.75 mm x 3.5 mm in width, length and height, respectively. This combustor is composed of a main channel, a cooling channel, flame holders, a combustion chamber and spark ignition plugs. Each layer is fabricated by MEMS processes, and is bonded together for assembling the combustor. As highlighted in the Fig.1, the air entered in the combustor is divided into two flows; main flow is for combustion in the chamber, and by-pass flow is for cooling the combustion chamber. The heat loss is reduced by the air flow in the cooling channel around the chamber. Fuel is injected through multiple fuel ports, and mixed with the air for combustion. The air-fuel mixture enters into the chamber through the flame holders, and is ignited by the spark plugs. Finally, the combustion gas is exhausted from the combustion gas exit. The air for cooling goes out from the cooling gas exit. Hydrogen (H_2) was selected as a fuel due to the wide flammability range, the low minimum ignition energy,

the high burning velocity, compared with the hydrocarbons [1-3].

3. COMBUSTION CHAMBER DESIGN

The combustion chamber is divided into two regions known as primary and secondary zones. As the intense backmixing is occurred in the primary zone, we can idealize this region as a Well-Stirred Reactor (WSR) from the viewpoint of chemical engineering. In a WSR, the volumetric mass rate of consumption of hydrogen RR_f is expressed by an Arrhenius equation for the overall combustion reaction [4],

$$RR_f = M_f A_r \exp\left(-\frac{E}{RT}\right)\left(\frac{p}{\bar{R}T\sum N_P}\right)^3 \phi^2(1-\varepsilon)^2(1-\phi\varepsilon), \qquad (1)$$

where M_f is the molecular weight of H_2, A_r is the pre-exponential factor, E is the activation energy of reaction, R and $\bar{R}$ are the universal gas constant(R =0.239$\bar{R}$), T is the static temperature of the air-fuel mixture, p is the static pressure of the mixture, $\sum N_P$ is the sum of the product mole numbers, ϕ is the equivalent ratio, and ε is the combustion efficiency. A simplified atom-balance equation is expressed by Eq.(2) on the assumption that the air is simply present as a diluent after forming H_2O for fuel-lean mixtures only.

$$\phi H_2 + \frac{1}{2}\left\{O_2 + \frac{79}{21}N_2\right\} \rightarrow \phi(1-\varepsilon)H_2 + \phi\varepsilon H_2O + \frac{1}{2}\left\{(1-\phi\varepsilon)O_2 + \frac{79}{21}N_2\right\} \qquad (2)$$

$\sum N_P$ is given by Eq.(3), using the right hand side of Eq. (2).

$$\sum N_P = \frac{50}{21} + \phi\left(1 - \frac{1}{2}\varepsilon\right). \qquad (3)$$

T is given by Eq.(4) from the energy balance equation in WSR.

$$T = T_i + \varepsilon(T_{AFT} - T_i) = T_i + \varepsilon\left(\frac{\phi f_{st} h_{PR}}{c_P}\right), \qquad (4)$$

where T_i is the combustor inlet temperature, T_{AFT} is the adiabatic flame temperature, f_{st} is the stoichiometric mass-basis fuel-air ratio, h_{PR} is the lower heating value of H_2, and C_p is the isobaric specific heat capacity of the mixture. RR_f can be expressed as a function of only ε by substituting Eqs.(3) and (4) into Eq.(1). Therefore, we can derive the value of ε that gives the maximum RR_f. This value of ε is expressed by ε_a.

RR_f is also represented as Eq. (5) with the conservation of mass in steady-flow WSR.

$$RR_f = \varepsilon\left(\frac{\phi f_{st}\dot{m}_E}{V_{WSR}}\right), \qquad (5)$$

where $\dot{m}_E$ is the mass flow entrained to the wake region in primary zone and V_{WSR} is the volume of the primary zone. By substituting the value of maximum RR_f and ε_a into Eq.(5), we can obtain the value of $\dot{m}_E/V_{WSR}$.

Here, the relationship of Eq.(6) has experimentally been confirmed [5].

$$\frac{\dot{m}_E}{\dot{m}_A} \propto \frac{U}{T_i^{0.75}}\frac{B_g}{(1-B_g)^{0.5}}, \qquad (6)$$

where $\dot{m}_A$ is the air flow of the mainstream entered into the chamber, U is the velocity of the mixture and B_g is the blockage ratio. As for the wake region in the combustion flow, it was reported that the wake region does not expand by twice or more the width of the flame holder [6]. Therefore, the WSR height is determined to be twice the width. From these considerations and Eq.(6), $\dot{m}_E/V_{WSR}$ is represented as Eq.(7)

$$\frac{\dot{m}_E}{V_{WSR}} = \frac{k\dot{m}_A^2}{2\rho T_i^{0.75}}\frac{\sqrt{mA_c}\left(A_c - mA_f\right)}{\left(mA_cA_f\right)^2}, \qquad (7)$$

where k is proportional constant determined by the shape of a flame holder, ρ is the density of mixture, A_c is the cross sectional area of the combustion chamber, A_f is a opening area of flame holder and m is the number of flame holders. We should design the primary zone with flame holders to correspond the value of

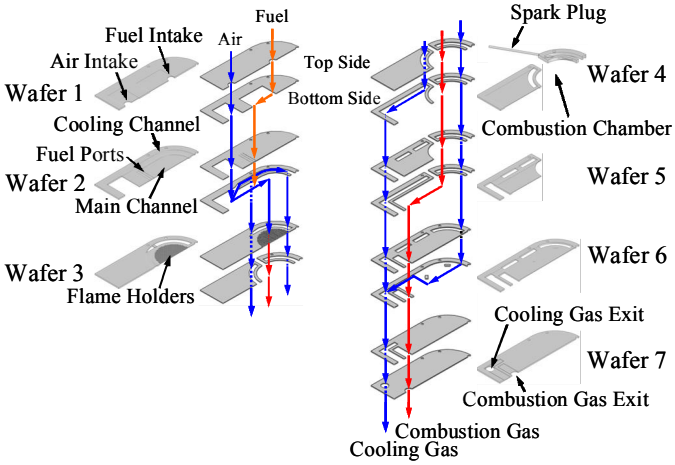

Fig.1 Schematic of micro combustor structure and gas passage.

$\dot{m}_E / V_{WSR}$ determined from Eq.(5) with the right hand side of Eq.(7).

The subsequent secondary zone is designed for spreading the flame to the entire mainstream. As shown Fig.2, the combustion chamber height is calculated from burning velocity, flow velocity and flame thickness. Since the burning velocity is always vertical to the flame sheet, the angle between the flow direction and the flame sheet is calculated from the burning and flow velocities. Height required for secondary zone can be calculated using this angle.

4. COMBUSTION TEST

Figure 3 shows the photograph of the micro combustor mounted on the fixture. In order to evaluate the performance of the micro combustor, the specific fixture was designed to connect the combustor to the large external instruments.

Before performing the combustion test, the ratio of total pressure loss (it is defined as the ratio of total pressure loss to total pressure at the combustor inlet) due to the combustor structure was measured. Seven layers model was evaluated in this experiment. Fig. 4 shows the ratios of total pressure loss at the combustion and cooling gas exits as a function of mass flow rate. These figures show that the ratios of total pressure loss are less than 4%, and good agreement with CFD analysis (SCRYU/Tetra ver.6). Thus, these results are acceptable for the required combustor specification.

In the combustion test, five layers model was used for measuring the temperature of the combustion chamber. Figures 5 and 6 depict the combustion chamber temperatures and combustion efficiencies as a function of equivalent ratio for different mass flow rates, respectively. The equivalent ratio is adjusted by the concentration of H_2. The experimental results show that a stable combustion has been sustained inside the chamber in a wide range of experimental conditions, and also combustion efficiency is 100% at the equivalent ratio from 0.4 to 0.5.

5. DISCUSSION

The parameter, known as "Air Loading I", can be derived from Eqs.(1) and (5),

$$I \doteq \frac{\dot{m}_E}{V_{WSR} P^3} = \frac{M_f A \exp\left(-\frac{E}{RT}\right)\phi(1-\varepsilon)^2(1-\phi\varepsilon)}{\varepsilon f_{st}\left(\overline{R}T\sum N_P\right)^3} . \qquad (7)$$

Though Eq.(7) can be used in the WSR region, Combustor Loading Parameter (CLP) can be obtained

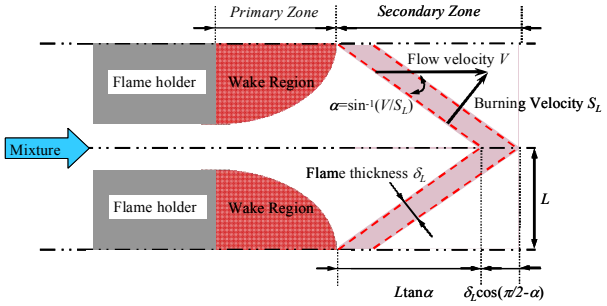

Fig.2 Schematic of the flame holders and the combustion chamber.

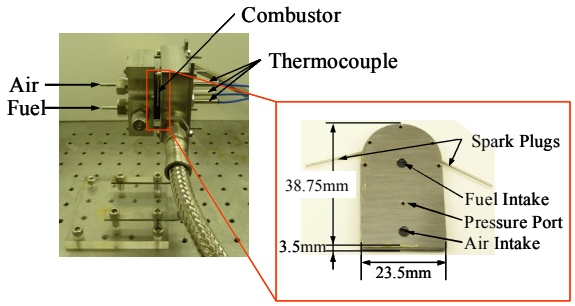

Fig.3 Photograph of the micro combustor mounted on the fixture

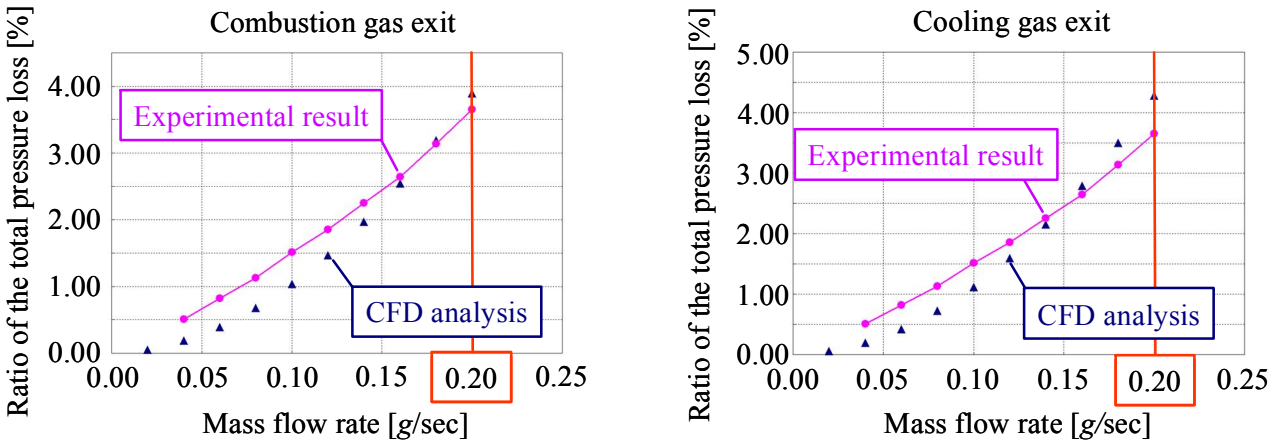

Fig.4 Ratios of total pressure loss at the combustion and cooling gas exits as a function of mass flow ratio.

by substituting of $\dot{m}_A$ into $\dot{m}_E$ and volume of combustion chamber V into V_{WSR}. The CLP is given by Eq.(8).

$$CLP \doteq \frac{\dot{m}_A}{VP^n} . \quad (8)$$

Figure 7 shows CLP as a function of the equivalent ratio for different mass flow rates. This figure is called the stability map of a combustor, and the validity has experimentally been confirmed as for the conventional large scale combustor [4]. It is reported that the experimental data are good agreement with the value when n is slightly less than exponent part in Eq.(7). In this paper, we used the value of n=3. Experimental results were plotted in Fig. 7, together with the numerical values of Eq.(8). As shown in Fig. 7, the points recorded as the stable combustion in this test is within the stable combustion of stability map. Therefore, the design using chemical reactor theory and stability map are effective in a micro combustor.

6. CONCLUSION

In this paper, we proposed a design of the micro combustor applying the chemical reactor theory used in the conventional combustor, and examined the validity of this method by hydrogen-air combustion test. The experimental results were plotted within the stable combustion of stability map for the micro combustor derived by the chemical reactor theory. These results are useful for a design consideration on the micro combustor.

REFERENCES

[1] C.M. Spadaccini, A. Mehra, J. Lee, X. Zhang, S. Lukachko and I.A. Waitz, 2003, High Power Density Silicon Combustion Systems for Micro Gas Turbine Engines, *Journal of Engineering for Gas Turbines and Power*, **vol. 125**, pp.709-719

[2] X.C. Shan, Z.F. Wang, Y.F. Jin, M. Wu, J. Hua, C.K. Wong and R. Maeda, 2005, Studies on a micro combustor for gas turbine engines, *J. Micromech. Microeng.*, **Vol. 15**, S215-S221

[3] Shuji Tanaka *et al.*, 2007, WORLD'S SMALLEST GAS TURBINE ESTABLISHING BRAYTON CYCLE, *Technical Digest PowerMEMS 2007 (Freiburg, Germany, 28-29 November 2007)*, pp.359-362

[4] Jack D. Mattingly, William H. Heiser, David T. Pratt, 2002, *AIRCRAFT ENGINE DESIGN SECOND EDITION* (American Institute of Aeronautics and Astronautics, Inc.)

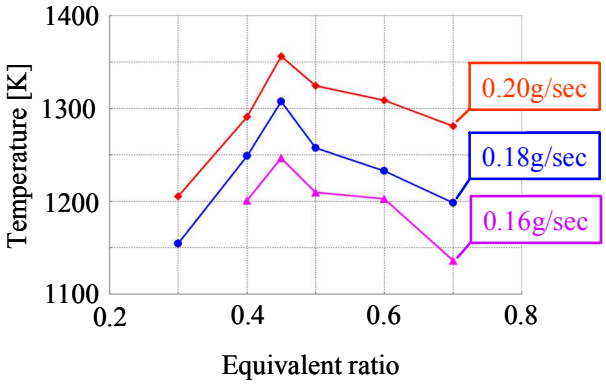

Fig.5 Combustion chamber temperatures as a function of equivalent ratios for different mass flow rate.

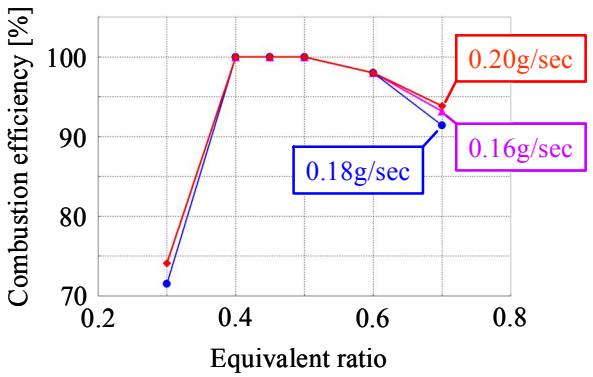

Fig.6 Combustion efficiencies as a function of equivalent ratios for different mass flow rate.

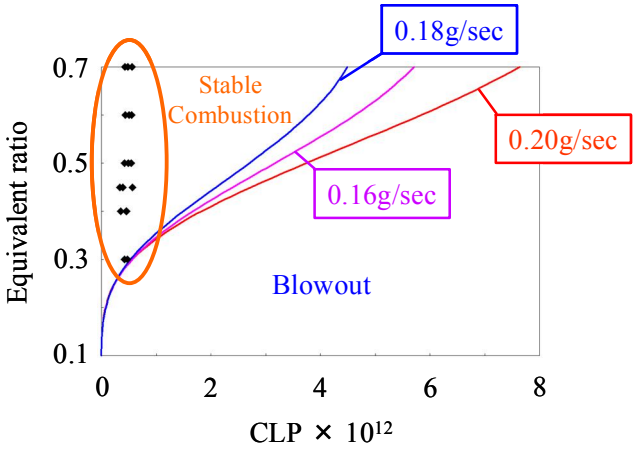

Fig.7 Stability map of a micro combustor.

[5] A. H. Lefebvre, A. R. A. F. Ibrahim, and N. C. Benson, 1966, Factors Affecting Fresh Mixture Entrainment in Bluff-Body Stabilized Flames, *Combust. Flame*, **vol. 10**, pp.231-239

[6] A. H. Legebvre, 1983, *Gas Turbine Combustion* (TAYLOR & FRANCIS)